



Deciduous dentition and dental eruption sequence of *Bothriogenys fraasi* (Anthracotheriidae, Artiodactyla) from the Fayum Depression, Egypt

Hesham M. Sallam, Afifi H. Sileem, Ellen R. Miller, and Gregg F. Gunnell

ABSTRACT

Paleogene anthracotheres are poorly documented from Afro-Arabian localities. This is due, in large part, to the fragmentary nature of the specimens that have been described. However, sediments in the Jebel Qatrani Formation, Fayum Depression, Egypt, preserve the richest anthracothere assemblage in all of Afro-Arabia. Unlike other samples, the Fayum collection includes many complete dentitions, skulls, and partial skeletons. Based on these extensive collections, this study provides the first description of the complete deciduous dentition and dental eruption sequence for the early Oligocene anthracothere *Bothriogenys fraasi*. A detailed discussion concerning the pattern and timing of dental growth in *B. fraasi* is provided, and the ontogenetic sequence documented for *B. fraasi* is compared with those available for suoids and hippos, the two extant groups currently considered as possible sister taxa to anthracotheres. Results show that anthracotheres and suoids share a more similar dental emergence pattern, and one that may be close to the primitive condition for artiodactyls, while hippos have a very different dental eruption sequence as a consequence of their highly divergent life history pattern. As a growing body of life history research indicates that taxa in close phylogenetic proximity may be expected to share features of their dental developmental pattern, this finding suggests a useful test of competing hypotheses of a relationship between Anthracotheriidae and either Hippopotamidae or Suiformes can potentially be developed based on eruption patterns.

Hesham M. Sallam, Mansoura University Vertebrate Paleontology Center, Department of Geology, Mansoura University, Mansoura, 35516, Egypt, and Department of Evolutionary Anthropology, Duke University, Durham, NC 27708, USA sallam@mans.edu.eg

Afifi H. Sileem, Vertebrate Paleontology Section, Cairo Geological Museum, Cairo, Egypt, afifi.sileem@yahoo.com

Ellen R. Miller, Department of Anthropology, Wake Forest University, Winston-Salem, NC 27106, USA, millerer@wfu.edu

Gregg F. Gunnell, Division of Fossil Primates, Duke Lemur Center, Durham, NC 27705, USA, gregg.gunnell@duke.edu

Keywords: Fayum; Egypt, Oligocene; juvenile; dentition; Artiodactyla

Submission: 13 February 2016 Acceptance: 16 August 2016

INTRODUCTION

The terrestrial mammal-bearing localities of the Jebel Qatrani Formation, Fayum Depression, Egypt, including the well-known quarries L-41, A, B, E, V, I, and M, are among the most productive Paleogene fossil localities known anywhere in Africa (Figure 1). The Jebel Qatrani deposits range in age from late Eocene through early Oligocene (~34 to ~30 Ma) (Kappelman et al., 1992; Seiffert, 2006; Seiffert et al., 2008), and fossils recovered from the Jebel Qatrani have profoundly influenced our understanding of primate (e.g., Seiffert et al., 2010; Seiffert, 2012), and mammalian evolution (e.g., Simons and Rasmussen, 1990; Simons, 2008). However, relatively few of these mammalian studies have focused on anthracotheres (Andrews, 1906; Schmidt, 1913; Black, 1978; Holroyd et al., 1996; Ducrocq, 1997; Sileem et al., 2015; Sileem et al., 2016), despite the fact that anthracotheres are among the most abundant fossils recovered from Fayum deposits.

Anthracotheriidae is an extinct family of artiodactyls known from Eocene – Miocene deposits across Laurasia and into Africa (but not elsewhere in Gondwana). Behaviorally, they are thought to have occupied a range of browsing niches over both their long temporal and broad geographic ranges, although whatever their specific feeding ecologies were they are widely acknowledged to have been semi-aquatic based on skeletal proportions and inferred habitats where fossils are found (e.g., Black, 1978; Pickford, 1991; Holroyd et al., 2010; Miller et al., 2014). As a group, identification of the closest living anthracothere relative within Artiodactyla is contested, with some researchers favoring a suiform affiliation (e.g., Pickford, 2007), and others supporting a closer relationship with extant Hippopotamidae (e.g., Black, 1978; Boissarie and Lihoreau, 2006; O’Leary et al., 2012).

Much of the recent work on anthracotheres has been concerned with establishing their alpha taxonomy, as reflected in observable differences

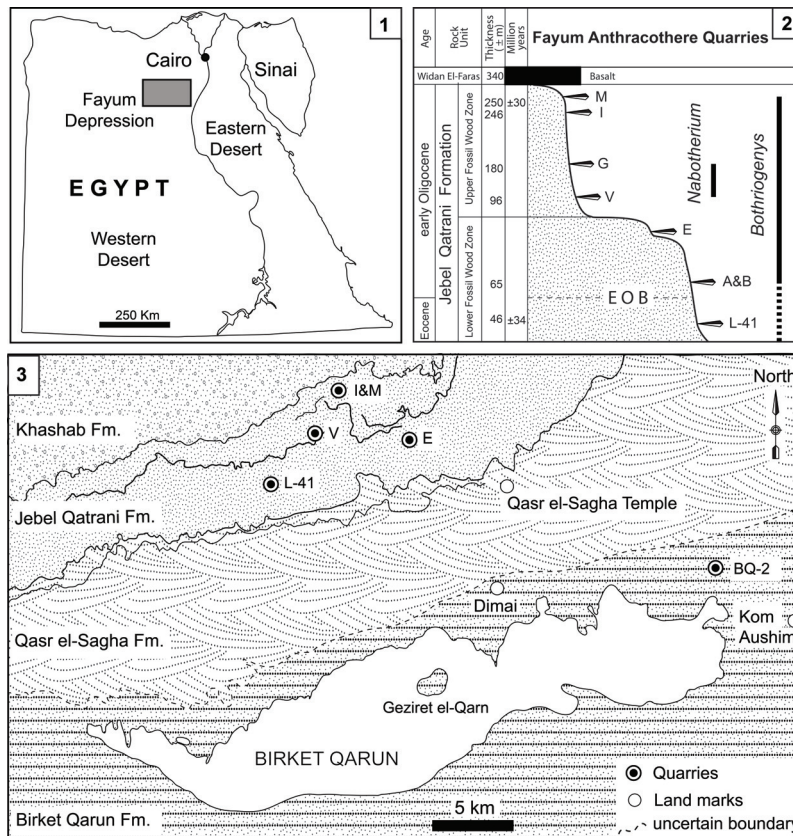


FIGURE 1. 1, location map of the Jebel Qatrani area, Fayum Depression. 2, stratigraphic positions and age estimates for major mammal-bearing fossil localities, following Seiffert (2006), EOB is abbreviation for Eocene Oligocene Boundary. 3, map of Jebel Qatrani area, showing different rock units, common landmarks and the approximate position of anthracothere-bearing fossil localities.

among adult dental morphologies (e.g., Lihoreau and Ducrocq, 2007, but for exceptions see Pickford, 2006; 2008). However, many of these investigations have been conducted without adequate material. The mandibular and maxillary material available in many museum collections preserves jaws with only molars and premolars, while many of the most striking differences among anthracothere taxa are manifest in their anterior dentition (e.g., presence/absence of diastemata, reduced v. caniniform canines, relative size, and orientation of incisors), even when the morphology of the cheek teeth remains more conservative.

In contrast, the collection of anthracothere material from the Jebel Qatrani Formation is comprised of a large number of anthracothere specimens (N= ~2270, including isolated teeth and postcranial elements), that are currently recognized as representing six species in three genera. A fairly large proportion of these preserve at least part of the anterior dentition and 12% (N=33/270) of the specimens attributed to *B. fraasi* are juveniles.

Here we provide the first documentation of the deciduous dentition and dental eruption sequence of the anthracothere, *Bothriogenys fraasi*, a taxon known from the early Oligocene upper sequence in the Jebel Qatrani Formation. This work represents the first detailed account of an ontogenetic sequence for any anthracothere taxon and is made possible by the decades of fieldwork in the Fayum that recovered such a large sample of remarkably well-preserved juvenile specimens. Results from this investigation into the pattern and timing of dental growth in *B. fraasi* will serve as a reference for comparison with other anthracothere species, and provides empirical information from growth and development towards resolving the phylogenetic relationships within anthracotheres, and between anthracotheres and other artiodactyl groups.

MATERIAL AND METHODS

Tooth position is referenced as dl, dC, dP, P, and M (for deciduous incisors, canine, premolars, and permanent premolars and molars, respectively), with upper and lower teeth designated by superscript and subscript numbers (respectively), such that, for example, dP⁴ is the fourth upper deciduous premolar. We follow the nomenclature of Bärmann and Rössner (2011) for dental features (cusps and crests) of upper and lower deciduous premolars (Figure 2).

In the following we refer to the first premolar of *Bothriogenys* as dP¹/₁. Based on the available

material, there is no evidence for P¹/₁ replacement suggesting that *Bothriogenys fraasi* retained a dP¹/₁ into adulthood. Morphology is not especially helpful to determine whether or not the retained tooth is deciduous or permanent because, unlike dP³/₃ and dP⁴/₄, dP²/₂ is neither molariform or of an exaggerated form but more like permanent P²/₂ suggesting that the first deciduous premolar would be simple as well.

It is not uncommon for mammals (some pigs, hippopotamus, horses, hyraxes) to retain deciduous first premolars that are not replaced (Zeigler, 1971; Lockett, 1993; Smith, 2000). Only *Tapirus* and maybe some archaeocete whales show evidence of replacement of the first premolar among mammals and in the case of the latter the evidence is not compelling (Lockett, 1993; Uhen, 2000). Therefore, the first upper and lower premolars of *Bothriogenys fraasi* are here considered to be retained deciduous teeth.

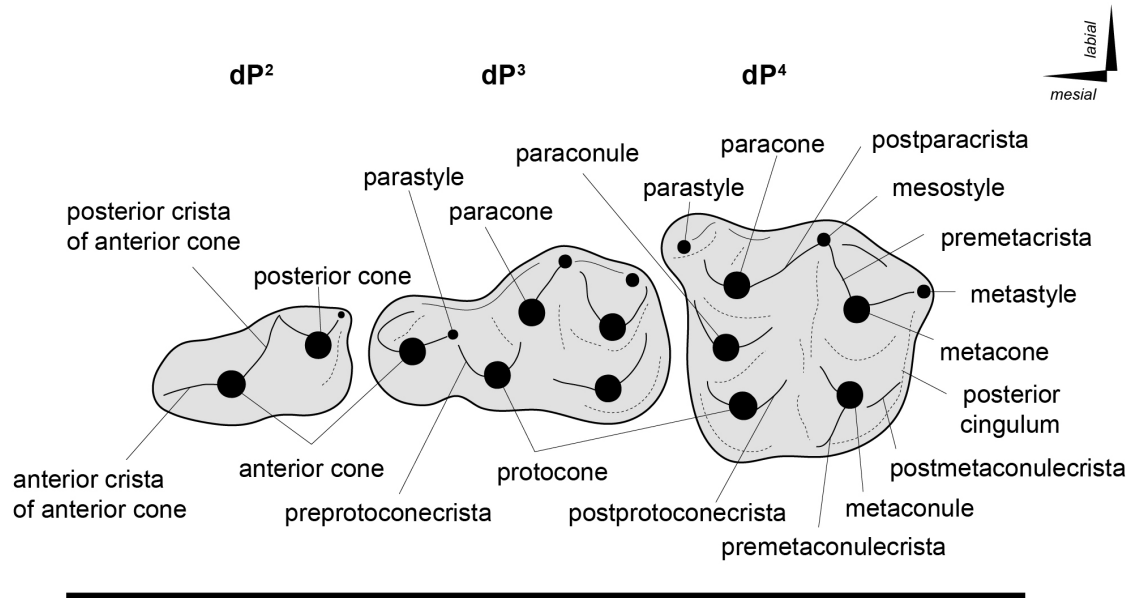
All specimens are cataloged in the Duke University Lemur Center, Division of Fossil Primates and designated with the prefix DPC. The studied materials were scanned using a Nikon XT H 225 ST micro-CT scanner housed at Duke University's Shared Materials Instrumentation Facility, and three-dimensional reconstructions were rendered in Avizo v.8. Dental measurements were taken from digital surface models (in Stanford "ply" format). All three dimensional (3D) digital materials are available for viewing and direct download at www.morphosource.org, (morphosource.org/index.php/Detail/ProjectDetail/Show/project_id/224). See also Table 1 for digital object identifiers, DOIs that directly link to 3D digital media associated with each specimen. More details yet are provided in Supplemental Material. Reuse of these data should cite MorphoSource, the DOI and this paper.

DESCRIPTION

Upper Deciduous Teeth

A complete upper and lower deciduous premolar dentition for *Bothriogenys fraasi* is available as a composite from specimens recovered from Fayum Quarries I, M, and O. DPC 5167 (Figure 3.1-4, Table 1) is a right maxillary fragment with light post-mortem distortion that has led to minor surface cracks and displacements. However, the specimen clearly preserves the alveolus for dP¹, and crowns of dP²-M¹, with M¹ half exposed. The upper deciduous second premolar in DPC 5167 is triangular, has two roots, and is separated from the mesial aspect of dP³ by a very short diastema. The

Upper deciduous premolars



Lower deciduous premolars

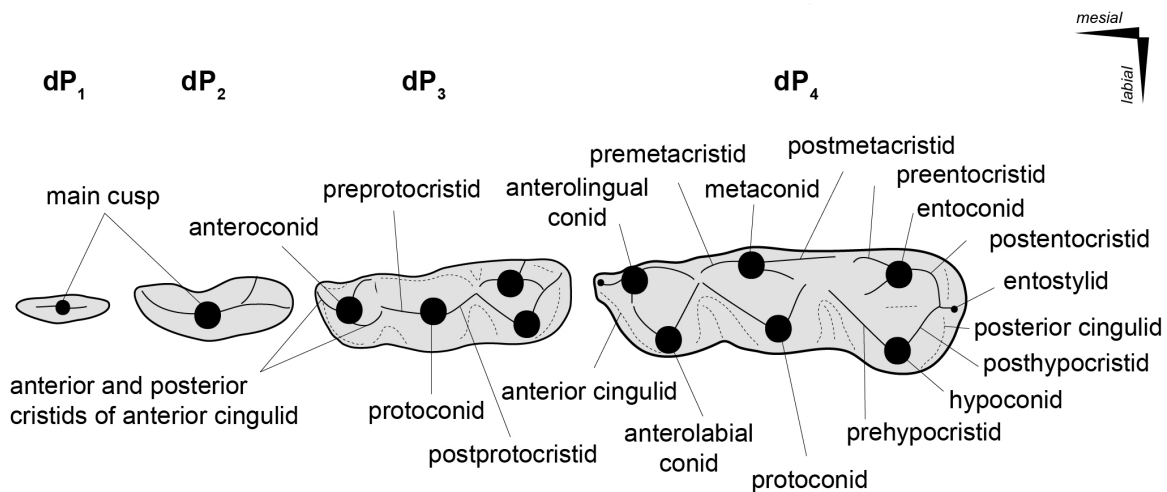


FIGURE 2. Dental terminology used to describe features of the deciduous premolars of *Bothriogenys fraasi*, following Bärmann and Rössner (2011).

crown of the tooth is convex labially and concave lingually, is longer than it is wide, and has an oval occlusal outline, owing to a slightly wider posterior region. The crown bears two main cusps, the anterior of which is larger and occupies the mesial part of the tooth, and the posterior cusp is smaller and occupies the distolabial portion of the crown. The anterior cusp has a pyramid shape with three crests, the mesial of which is curved and joins a very short and low antero-cingulum. The distolabial crest of the anterior cusp is longer than the mesial crest, and slopes down to meet the mesial crest of

the posterior cusp, creating a small inverted V-shape on the labial border of the tooth. The distolingual crest of the anterior cusp is straight and short and runs distolingually. The distal crest of the posterior cusp has the same length as the mesial crest, and runs distally to end as a small projection in the distolabial corner of the crown. There is a low and weakly developed but broad cingulum extending around the lingual margin of the posterior cusp that connects distally with the distal crest of the posterior cusp, and joins the distolingual crest of

TABLE 1. Length and width of teeth (in millimeters) of juvenile specimens of *Bothriogenys fraasi* from the upper most terrestrial mammal-bearing localities of the Jebel Qatrani Formation, Fayum Depression, Egypt. DOIs representing microCT data and associated mesh files and photographs on MorphoSource. The DOIs can be also found in Table S1 and should be cited along with this paper and MorphoSource if reused.

<i>Bothriogenys fraasi</i>											
Upper		dP ¹		dP ²		dP ³		dP ⁴		M ¹	
DPC 3224 doi.org/10.17602/M2/M12690	Right	--	--	--	--	--	--	15.13	15.55	--	--
DPC 5167 doi.org/10.17602/M2/M12646	Right	--	--	11.22	5.18	15.21	10.40	15.00	13.66	18.90	?
DPC 20439 doi.org/10.17602/M2/M12647	Right	--	--	--	--	16.27	10.65	15.29	14.40	--	--
Lower		dP ₁		dP ₂		dP ₃		dP ₄		M ₁	
DPC 2705 doi.org/10.17602/M2/M12688	Right	--	--	8.86	4.35	16.25	6.89	21.93	9.17	20.82	11.77
DPC 3606 doi.org/10.17602/M2/M12653	Right	--	--	--	--	17.17	6.29	21.49	8.59	--	--
DPC 3947 doi.org/10.17602/M2/M12639	Left	--	--	--	--	17.03	6.23	21.40	8.69	--	--
DPC 6147 doi.org/10.17602/M2/M12649	Left	--	--	--	--	--	--	20.45	8.23	--	--
DPC 7706 doi.org/10.17602/M2/M17034	Right	--	--	8.26	4.08	17.76	6.47	21.56	8.72	20.18	11.81
DPC 7730 doi.org/10.17602/M2/M12655	Left	--	--	9.43	4.41	17.77	6.94	22.54	9.16	21.48	12.15
DPC 8638 doi.org/10.17602/M2/M12684	Right	--	--	7.91	4.05	15.75	6.26	20.31	7.99	19.08	10.29
DPC 10616 doi.org/10.17602/M2/M12650	Left	--	--	--	--	--	--	20.32	7.66	19.41	10.20
DPC 10633 doi.org/10.17602/M2/M12654	Right	--	--	--	--	15.72	5.77	20.27	7.93	--	--
DPC 11280 doi.org/10.17602/M2/M12645	Left	--	--	--	--	--	--	21.24	8.44	19.15	10.64
DPC 11407 doi.org/10.17602/M2/M12651	Left	--	--	--	--	--	--	20.38	8.18	18.68	10.63
DPC 11412 doi.org/10.17602/M2/M12648	Right	--	--	--	--	15.11	6.51	21.50	8.41	--	--
DPC 11416 doi.org/10.17602/M2/M12641	Left	7.01	2.96	9.20	4.67	16.87	6.54	22.63	8.83	--	--
DPC 13570 doi.org/10.17602/M2/M17039	Left	--	--	9.27	4.30	16.05	6.33	21.17	8.46	--	--
DPC 13562 doi.org/10.17602/M2/M12638	Right	--	--	--	--	15.22	6.07	21.26	8.58	19.06	10.71

the anterior cusp mesially. The dP² is the least worn of the upper deciduous dentition.

The dP³ is well-preserved in DPC 5167 and DPC 20439 (Figure 3.1-5). The dP³ is longer than wide, and has a roughly triangular outline with a narrower anterior portion and a broader posterior one. The occlusal surface has five major cusps (anterior cone, protocone, paracone, metacone, and metaconule), all of which are more or less equal in size, and all of which are about the same height, except for the paracone, which is some-

what smaller. The anterior cone occupies the most mesial portion of the crown and bears three crests. The lingual crest originates at the apex and runs lingually, curving distally to end at the base of the protocone and so enclosing a lingual anterior valley. There are two labial crests running from the anterior cone, which together delimit a small fovea on the labial border of the anterior cone. The protocone is the highest cusp in the crown and is situated distal to the anterior cone. The protocone has a conical shape with a mesial crest that joins the

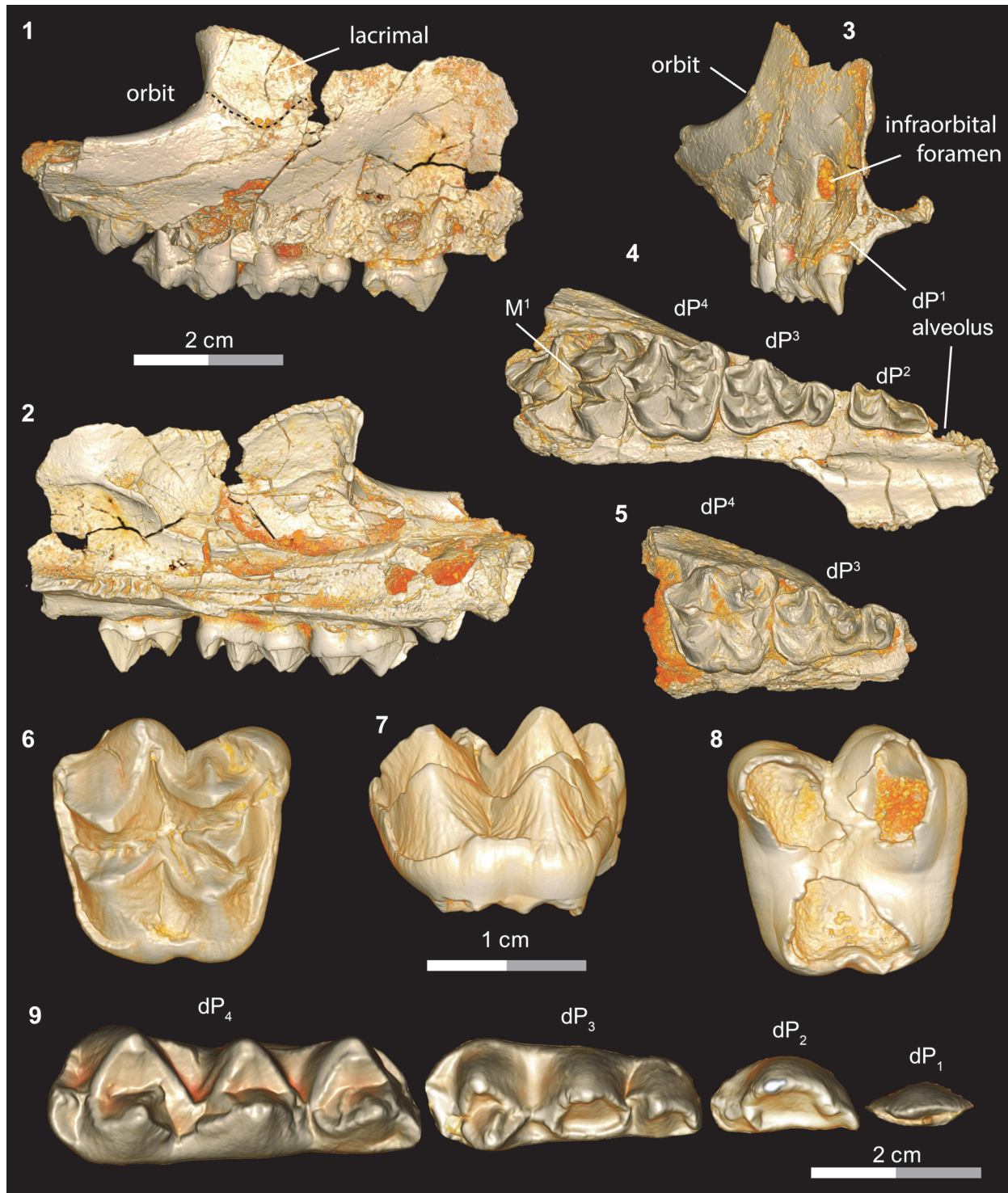


FIGURE 3. 1-4, right partial maxilla of DPC 5167 with dP²-M¹, in (1) lateral, (2) medial, (3) anterior, and (4) occlusal views; 5, right partial maxilla of DPC 20439 (doi.org/10.17602/M2/M12647) with dP³- dP⁴, in occlusal view; 6-8, right dP⁴ of DPC 3224 (doi.org/10.17602/M2/M12690), in (6) occlusal, (7) lingual, (8) ventral views; 9, DPC 11416 (doi.org/10.17602/M2/M12641) with dP₁- dP₄, in occlusal view.

distal crest of the anterior cone at a level lower than the apex, creating a V-shaped crest that helps close the anterior valley labially. The postparacrista slopes down distolabially to merge with the mesostyle, and the premetacrista slopes down mesolabially to connect with the mesostyle. Together these crests form an inverted V-shape that protrudes as a mesostyle and weakly closes the posterior valley labially. The mesostyle is crestiform, weakly developed, and has a worn surface on both specimens. The metacone is pyramid shaped and bears three crests, the distal of which runs distally and interrupts the posterior cingulum. The premetacrista is the mostly heavily worn crest on the crown. The metaconule is transverse to the metacone and connected to it via a short crest. The postmetaconulecrista runs distolabially and ends at the midpoint of the posterior cingulum. The premetaconulecrista runs mesially and terminates at the base of the protocone, closing the posterior valley lingually. The posterior valley of dP³ is broader and longer than the anterior valley. The posterior cingulum is relatively well developed, in particular the labial aspect and starts from the base of the mesostyle, courses around the posterior margin of the tooth, and terminates at the base of the protocone.

The dP⁴ occlusal surface is nearly identical to that of the first upper molar, differing only in being relatively smaller and having less robust cusps and crests. DPC 3224 (Figure 3.6-8) is the most well-preserved dP⁴ in the available material. The dP⁴ has a semi-quadrate outline and four main cusps (paracone, protocone, metacone, and metaconule), all of which are about equal in size. The mesostyle is well developed, placed slightly distal of center on the labial wall of the tooth, and extends farther labially than the parastyle. The lingual side of the mesostyle is invaded by the postparacrista and premetacrista, extending the profossa labially in a V-shape between the paracone and metacone. There is no cingulum that runs distally from the mesostyle to meet the postmetacrista as is seen in M¹. The parastyle is distinct and crestiform and forms the mesiolabial corner of the crown. The paraconule is distinct, triangular in shape, and situated at the midpoint between the paracone and the protocone, from which it is separated by deep, narrow notches. The preparacristule runs down mesiolabially toward the base of the paracone, whereas the postparacristule runs distally and fades before reaching the main valley of the crown. The preprotocrista is short and runs mesially to connect with the lingual

base of the paraconule, and there are two postprotocristae that run distolabially. The metaconule bears three cristae; the premetacristule runs mesiolabially toward the main valley and connects with the most lingual postprotocrista, interrupting the course of the main valley. The postmetacristule is well developed, runs distolabially, and fuses with the distal cingulum. The lingual metacristule becomes a continuation of the mesial portion of the lingual cingulum. The distal cingulum is moderately developed, extends lingually, and courses around the lingual base of the metaconule, forming the distal portion of the lingual cingulum. The mesial cingulum is well developed but low, and runs lingually from the parastyle. In DPC 5167, the cingulum courses around the lingual base of the protocone and merges with the lingual metacristule, while in DPC 3224 and 20439, the cingulum terminates at the mesial base of the protocone. The main valley is closed lingually either via a low connection between the base of the protocone and the metaconule, or by a continuous lingual cingulum.

Lower Deciduous Teeth

DPC 11416 (Figures 3.9, 4) preserves the complete lower deciduous premolars series (dP₁₋₄) and several other juvenile mandibular specimens of *Bothriogenys fraasi* preserve parts of the deciduous series (Table 1).

The dP₁ is visible in DPC 11416 but the tooth is not completely erupted. The dP₁ is a small, peg-like tooth, with a labiolingually compressed crown and an oval base. The dP₁ crown has one main cusp, from which run mesial and distal cristids, the distal one being longer than the mesial one. The tooth is single-rooted, convex laterally, concave medially, and curves distally.

The dP₂ is a double-rooted tooth with one main cusp that has its apex in the middle of the crown. The tooth has a triangular shape in lateral view. The labial surface of the crown is convex, and the lingual surface is concave. The crown bears two main cristids. The distal cristid in some cases branches into two cristids, leading to a relatively narrow groove. On the distal border, there is a weakly developed cingulid that extends mesially onto the lingual border of the crown.

The dP₃ is double-rooted molariform with a crown length greater than width and has a generally rhomboidal outline. The occlusal surface is occupied by four major cusps (anteroconid, protoconid, entoconid, and hypoconid). The anteroconid is concave lingually and convex labially. In some cases, it bears three cristids, the two mesial ones

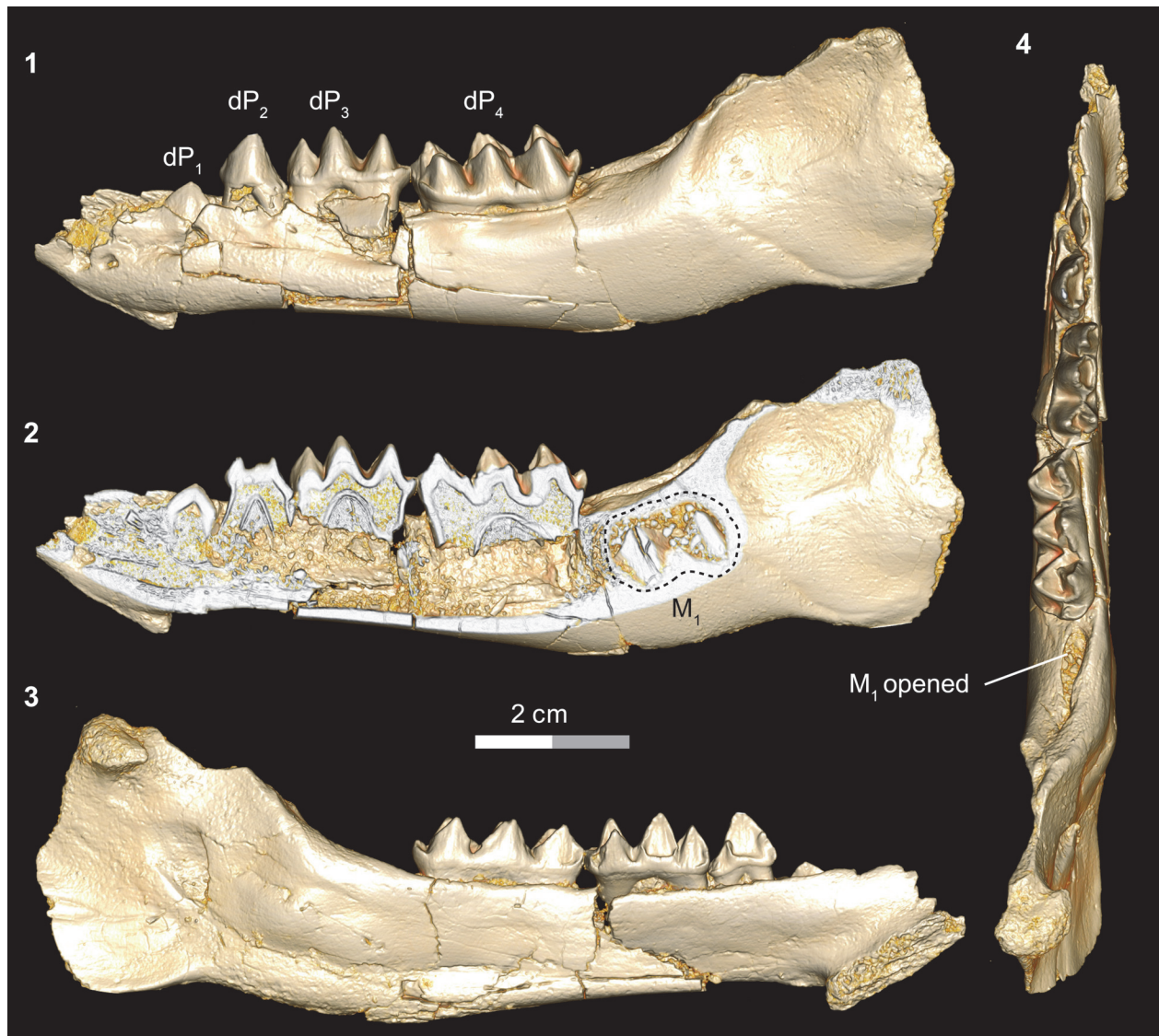


FIGURE 4. Left mandibular fragment of DPC 11416 (doi.org/10.17602/M2/M12641) with dP₁- dP₄, showing stage I of the eruption sequence of *Bothriogenys fraasi*, in (1) lateral, (2) internal, (3) medial, and (4) occlusal views.

of which delimit a small depression similar to the corresponding fovea on the dP³. The mesial cristid of the anteroconid slopes down toward the mesiolingual corner of the crown and forms the very mesial tip of the tooth. The distal cristid of the anteroconid is relatively weakly developed when compared with the mesial cristid. The labial cingulid is low and well developed, and runs from the labial base of the protoconid coursing around the anteroconid (in some specimens), and meets with the distal cristid of the anteroconid. The protoconid is the largest and tallest cusp and is situated distal to the anteroconid, from which it is separated by a narrow and deep notch. The labial side of the protoconid is concave, and the lingual side is some-

what convex, with low and well-developed lingual cingulid. The hypoconid is relatively large, occupies the distolabial corner of the crown, and has relatively well-developed prehypocristid and posthypocristid, which run mesiolingually and distolingually, respectively, from its tip. The entoconid is the smallest cusp and it is positioned transversely relative to the hypoconid, from which it is separated by a deep and narrow valley. The preentocristid meets the prehypocristid mesially, both of which join the postprotocristid at the posterior valley. The postentocristid runs distolabially from the entoconid to connect with the posthypocristid distally, and both continue as a single cristid that connects to the distal cingulid, forming the distal tip of the

crown. In some specimens, the entoconid lacks a postentocristid. The distal cingulid is relatively broad and limited to the posterior border of the tooth.

The dP_4 is larger than dP_3 , it is longer than it is wide, and the tooth is rhomboidal in occlusal outline, with a wide talonid and a narrow trigonid. The tooth bears six major cusps (anterolingual conid, anterolabial conid, metaconid, entoconid, protoconid, and hypoconid). On the occlusal surface, the lingual cusps align mesodistally, and are slightly higher than the labial cusps. The mesial sides of the latter cusps show some wear in specimens of more advanced aged. On the lingual border of the tooth, there are two deep V-shaped notches separating the lingual cusps, while on the labial border, two wide and deep sinuses separate the labial cusps. The entostylid is distinct and the smallest cusp of the crown. The anterolingual conid is placed mesial to the anterolabial conid, from which it is separated via a narrow and deep notch. The cusp has three cristids, the most mesial of which runs mesiolingually, forming the mesial tip of the crown. The labial cristid of the anterolingual conid runs mesiolabially to join the mesial cristid of the anterolabial conid, forming a V-shape at the mesiolabial corner of the crown. The distal cristid is directed toward the base of the metaconid. The anterolabial conid has two cristids, the distal cristid of which slopes down distolingually to attach to the junction of the preprotocristid, the premetacristid, and the distal cristid of mesiolingual conid. The metaconid has three cristids (mesial, distal, labial), is situated transverse to the protoconid, and is separated from the protoconid by a deep, narrow valley. The postprotocristid meets with the labial cristid of the metaconid at a high level on the crown. The postmetacristid is distally oriented and slopes down from the tip of the cusp to reach the distal basin of the crown. The entoconid has three main cristids; the preentocristid slopes down from the tip of the tooth to end at the base of the postmetacristid, leaving the distal basin open lingually; the postentocristid is directed distally and curves to connect with the posthypocristid, forming a V-shape and closing the basin between hypoconid and entoconid distally; the labial cristid of the entoconid runs mesiolabially and ends at the base of the hypoconid. The prehypocristid is well developed and slopes down from the hypoconid toward the junction between the postprotocristid and the postmetacristid. The distal cingulid is well developed but short, and bears a distinct small entostylid, which is connected mesially with the tip of

the distal V-shape pattern of the tooth via a short crestid.

TOOTH ERUPTION SEQUENCE AND COMPARISONS

A nearly complete lower tooth eruption sequence can be documented for *Bothriogenys fraasi* (Figures 4, 5, 6, 7, 8, Table 2). This eruption sequence can be compared with that of the extant *Hippopotamus* (Laws, 1968), and the European wild boar *Sus scrofa* (Matschke, 1967). Information about the dental eruption sequence for both taxa is available, and both taxa represent higher level groups that have been frequently cited as being sister taxa to or derived from anthracotheres (Geisler and Uhen, 2003; Pickford, 2008; Boisserie et al., 2010; Lihoreau et al., 2015).

In the developmentally earliest stage (Figure 4.1-4), *Bothriogenys fraasi* exhibits an exposed dP_1 crown tip, a nearly completely erupted dP_2 , fully erupted dP_{3-4} , and an M_1 visible in the crypt but not yet having begun to erupt. There is no evidence of a C_1 - dP_1 diastema at this point, which must represent a very early post-partum stage. This stage roughly corresponds to Laws' (1968) *Hippopotamus* groups I and II, which he interprets to represent ages between birth and six months, respectively. Laws (1968) noted that in hippos only the second through fourth deciduous premolars were replaced but that there was no evidence that the first deciduous premolar was replaced, only lost through ontogeny.

There are some differences between *Bothriogenys* and *Hippopotamus* during these early stages of development. The first deciduous premolar in *Hippopotamus* erupts before dP_2 , while it has clearly just begun to erupt when dP_2 is nearly fully erupted in *Bothriogenys*. As in *Hippopotamus*, dP_1 is not replaced in *Bothriogenys* (or in any other Fayum anthracothere for which there is data) but unlike *Hippopotamus*, *Bothriogenys* does not lose dP_1 later in ontogeny, typically retaining it throughout life.

When compared with *Sus*, *Bothriogenys* stage I roughly corresponds to the documented sequence of eruption for the extant taxon but there are differences. *Bothriogenys* stage I documents the beginning of eruption of dP_1 , full eruption of the other three deciduous premolars, and M_1 has yet to appear. In *Sus*, following the full eruption of dP_{2-4} (which occurs by 100 days), M_1 is in place at ~172 days followed by P_1 (or dP_1) at ~204 days. Thus, the first permanent molar erupts before P_1 (or dP_1)

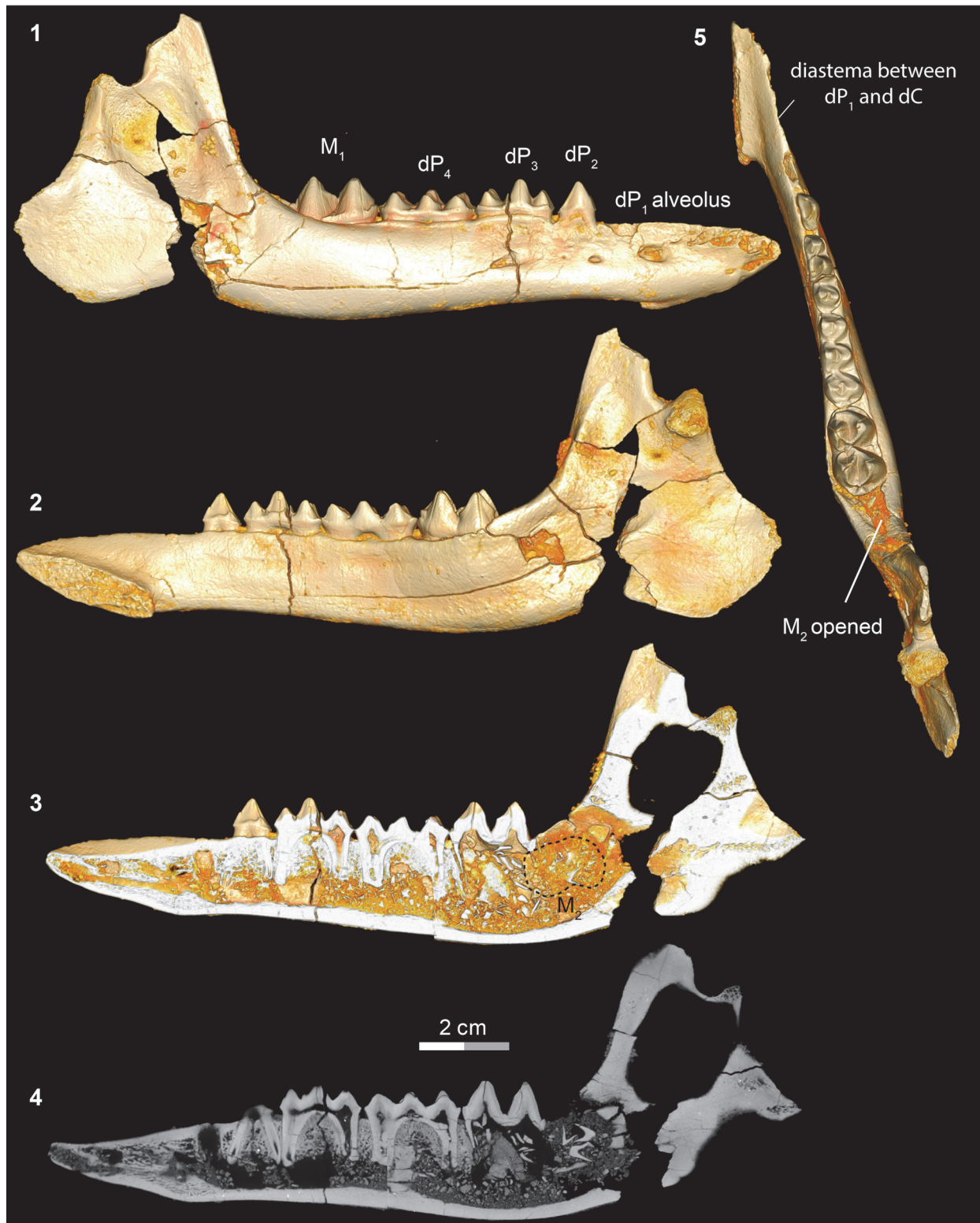


FIGURE 5. Right mandibular fragment of DPC 7706 (doi.org/10.17602/M2/M17034) with dP₂-M₁, showing stage II of the eruption sequence of *Bothriogenys fraasi*, in (1) lateral, (2) medial, (3-4) internal, and (5) occlusal views.

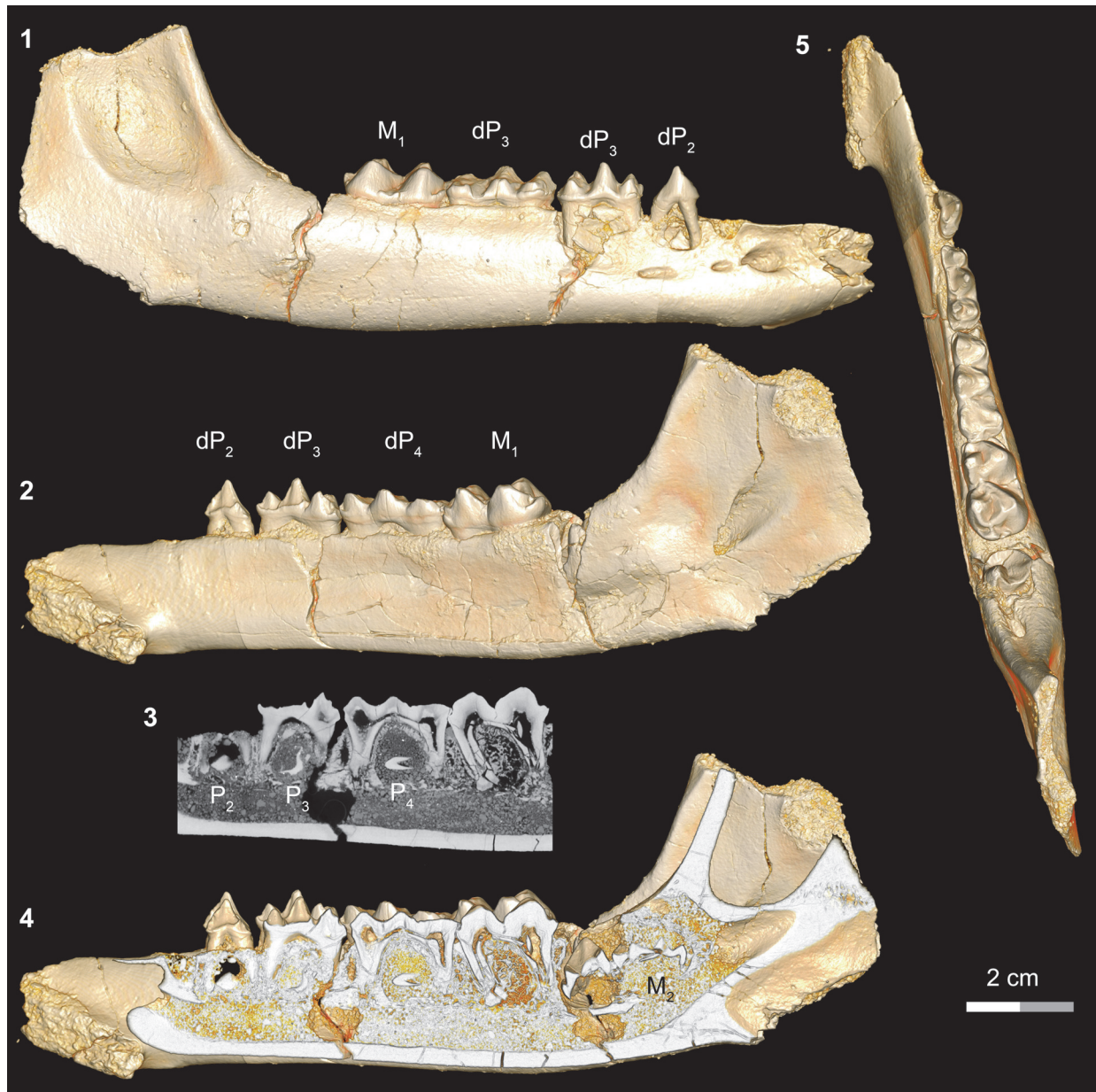


FIGURE 6. Right mandibular fragment of DPC 2705 (doi.org/10.17602/M2/M12688) with dP₂- M₁, showing stage III of the eruption sequence of *Bothriogenys fraasi*, in (1) lateral, (2) medial, (3-4) internal, and (5) occlusal views.

in *Sus* while the opposite is true in *Bothriogenys*. *Bothriogenys* stage I also shows no wear on the deciduous premolars.

Stage II in *Bothriogenys* (Figure 5) documents the beginning of the development of the C₁-dP₁ diastema and roughly corresponds to Laws' (1968) *Hippopotamus* group III, which occurs at approximately one year of age. In *Bothriogenys*, dP₁₋₄ are fully erupted as is M₁, while M₂ is just appearing in the crypt but has not yet begun to erupt, and there is no opening on the surface of the mandible to

indicate its presence. As in *Hippopotamus*, dP₄ shows relatively heavy wear at this stage but unlike in *Hippopotamus* dP₃ remains unworn in *Bothriogenys*. In *Sus*, the equivalent of *Bothriogenys* stage II is reached by an age of about 33 weeks (roughly six months of age).

Stage III in *Bothriogenys* (Figure 6) shows the continuation of mandibular growth as the C₁-dP₁ diastema approaches adult length. The early beginning of crown formation for permanent P₂₋₄ can be seen in scanned images and their apices

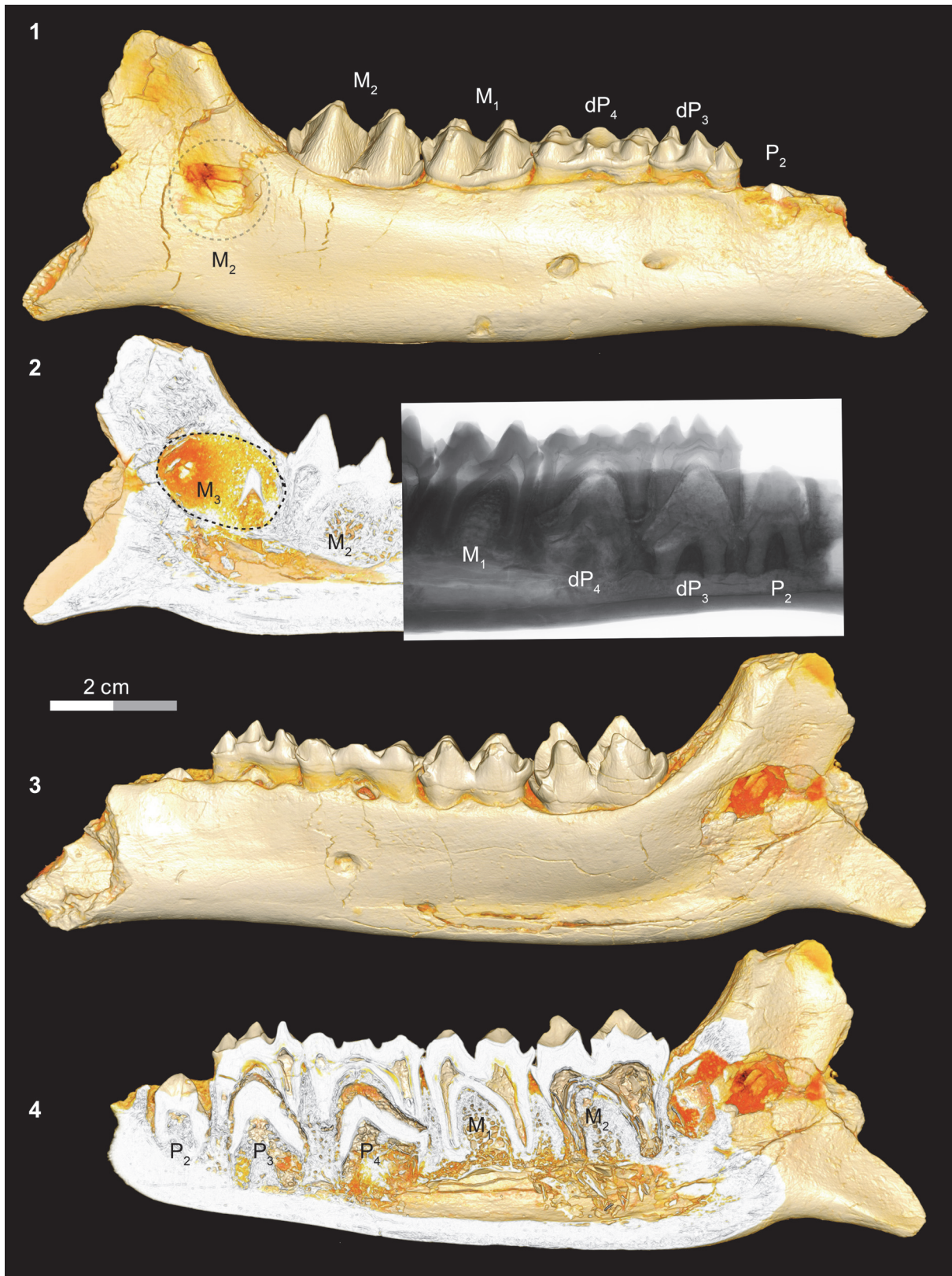


FIGURE 7. Right mandibular fragment of DPC 13562 (doi.org/10.17602/M2/M12638) with P₂, dP₃₋₄, M₁-M₂, showing stage IV of the eruption sequence of *Bothriogenys fraasi*, in (1) lateral, (2, 4) internal and X-ray, and (3) medial views.

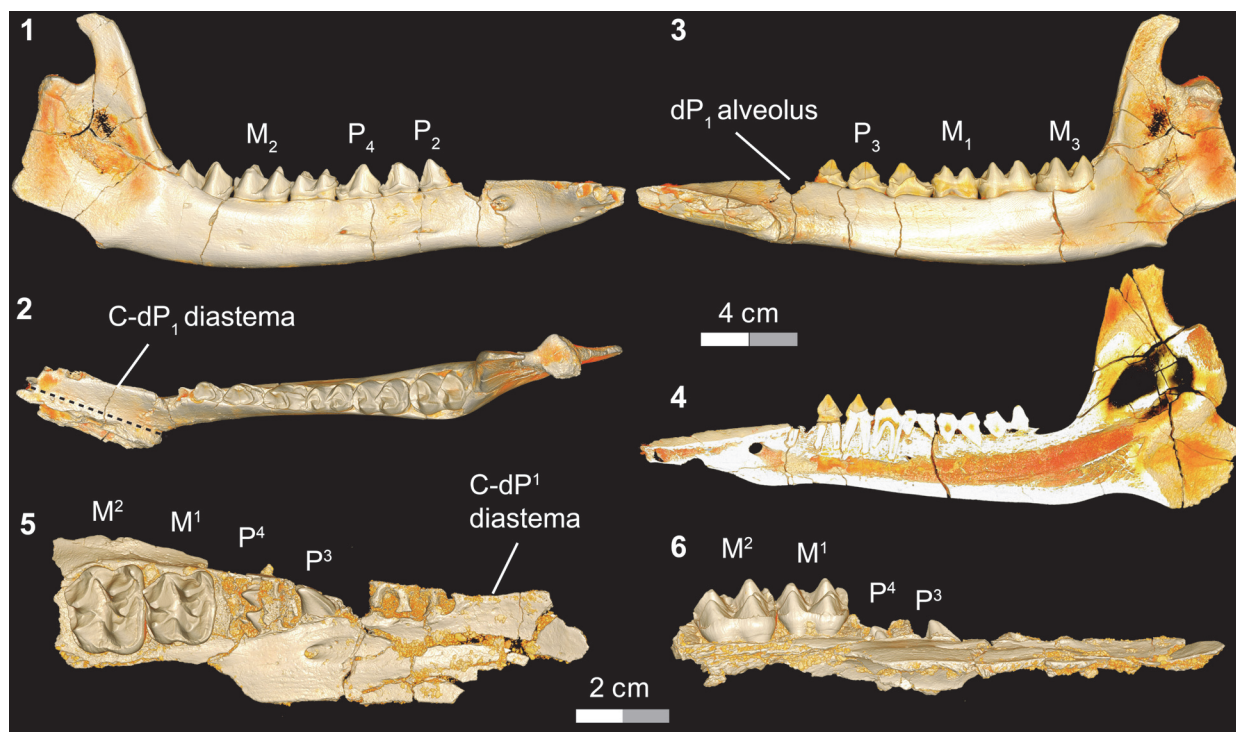


FIGURE 8. Right mandibular fragment of DPC 6207 (doi.org/10.17602/M2/M17032) with P₂- M₃, showing stage V of the eruption sequence of *Bothriogenys fraasi*, in (1) lateral, (2) occlusal, (3) medial, (4) internal views; 5-6, right partial maxilla of DPC 10677 (doi.org/10.17602/M2/M12698), in (5) occlusal and (6) medial views.

point horizontally. The M₂ crypt is open on the mandibular surface so that M₂ is visible. This stage corresponds roughly to Laws' (1968) *Hippopotamus* groups IV and V (ages three to four years, respectively). Like in *Hippopotamus* group IV, dP₃, and dP₄ both show relatively heavy wear, and M₁ has also begun to wear but M₂ is not visible on the mandibular surface in *Hippopotamus* group IV. By *Hippopotamus* group V, the M₂ is visible in its crypt but this group differs from *Bothriogenys* stage III in having both permanent P₂ and P₃ visible on the surface whereas they have barely begun to form in *Bothriogenys*. This stage corresponds to roughly one year of age in *Sus* (Matschke, 1967).

In *Bothriogenys* stage IV (Figure 7) permanent P₂ is now exposed on the surface, P₃ and P₄ have not yet begun to erupt but their crowns are fully formed beneath dP₃₋₄, M₁₋₂ are fully erupted, and M₃ is visible in its crypt. There is moderate to heavy wear present on dP₃₋₄ and M₁, but M₂ remains unworn or only slightly worn at this stage. This stage corresponds to *Hippopotamus* groups VII and VIII (ages 8 to 11 years, respectively) as documented by Laws (1968). The main differences with *Hippopotamus* are that *Bothriogenys* has not

erupted permanent P₂₋₄ yet but does have a fully erupted M₂, which does not occur in *Hippopotamus* until group VIII. By *Hippopotamus* group VIII, only dP₄ remains from the deciduous dentition, dP₁ is lost (may happen as early as group VI), and M₃ is still not visible on the surface of the mandible.

Bothriogenys stage IV documents an eruption pattern similar to that seen in *Sus*. At this stage, *Bothriogenys* has P₂ erupting but retains dP₃₋₄ and has a fully erupted M₁₋₂. In *Sus*, at the point where M₂ is fully erupted (at ~385 days) dP₂₋₄ are still retained, and there are no signs of permanent premolars (except for P₁) or M₃. In *Sus* the permanent premolars are fully erupted by ~490 days.

Stage V in *Bothriogenys* (Figure 8) documents the appearance of the full adult dentition and the completion of mandibular growth wherein the C₁-dP₁ diastema reaches its maximum length. DPC 10677, right partial maxilla with P₂-M₁₋₂, shows that P₃ and P₄ are exposed simultaneously, which represents the early phase of stage V. At this stage only M₁ exhibits moderate wear, while all other cheek teeth essentially have no evidence of wear. This stage is reached by group XII in *Hippopotamus*, which occurs at 22 years. At this point in *Hip-*

TABLE 2. Juvenile dental eruption sequence of *Bothriogenys fraasi* from the upper most terrestrial mammal-bearing localities of the Jebel Qatrani Formation, Fayum Depression, Egypt.

Eruption stage	Eruption sequence of <i>Bothriogenys fraasi</i> juveniles	Specimen no.	Quarry
Stage I	dP ₁ exposed; dP ₂ , dP ₃ and dP ₄ erupted; M ₁ opened	DPC 3606	M
		DPC 3947	M
		DPC 11416	I
		DPC 13570	I
		DPC 16633	I
Stage II	dP ₁ exposed; dP ₂ , dP ₃ , dP ₄ , M ₁ erupted; M ₂ opened	DPC 7706	M
		DPC 8638	M
		DPC 11280	M
		DPC 11407	M
Stage III	P ₃ and P ₄ start to form; dP ₃ , dP ₄ , M ₁ present; M ₂ exposed	DPC 2705	M
		DPC 7730	I
		DPC 10616	O
Stage IV	P ₂ exposed; P ₃ and P ₄ formed; dP ₃ , dP ₄ , M ₁ , M ₂ present M ₃ opened	DPC 13562	I
Stage V	Adult form i with P ³ and P ⁴ half exposed	DPC 10677	I
	Adult form ii with M ₃ half exposed	DPC 6207	I
	Adult form iii with M ₃ fully exposed	DPC 20950	M

popotamus, M₁ and M₂ are exhibiting heavy wear and cusp tips are beginning to wear on P₂₋₄ and M₃. In *Sus*, a fully adult dentition is acquired by ~755 days with the eruption of M₃.

DISCUSSION AND CONCLUSIONS

From the previous description, it is clear that the *Bothriogenys* tooth eruption sequence (Figure 9) differs from both those of *Hippopotamus* and wild boars (*Sus*). The main difference with *Hippopotamus* is that the anthracothere retains all deciduous premolars through the period when the third molar becomes visible in its crypt on the mandibular surface. Only the crown of permanent P₂ becomes visible at the end of this sequence (Figure 9, Stage IV). In *Hippopotamus*, no deciduous premolars remain by the time M₃ has appeared in its crypt on the mandibular surface, and all three permanent premolars (and dP₁) are fully erupted. With regard to the overall sequence of premolar versus molar eruption, *Bothriogenys* is more similar to *Sus* than it is to *Hippopotamus*, except for the sequence of erupting the first deciduous premolar

before M₁ in *Bothriogenys*, and *Sus* doing the opposite.

It is unclear why *Hippopotamus* exhibits an accelerated eruption of its permanent premolars relative to that seen in *Bothriogenys* and *Sus*, however, this is a somewhat common phenomenon in longer lived species Smith (2000), referred to the pattern of permanent teeth erupting earlier in more slow growing, longer-lived species as Schultz's Rule. She found evidence to support Schultz's Rule across a broad array of mammalian taxa including many species of ungulates, hippopotamus among them. Based on Smith's 2000 study, it is reasonable to postulate that artiodactyl groups that show this shift in eruption patterns (such as that seen in *Hippopotamus*) may represent a specialization within the order. Slower loss of the deciduous cheek tooth dentition (relative to permanent tooth eruption) therefore may be primitive for artiodactyls, given that both *Bothriogenys* and *Sus* exhibit this pattern.

Part of the explanation for these differences in eruption pattern probably has to do with differences in longevity as suggested by Schultz's Rule (Smith, 2000). Based on differences in body mass (Eisen-

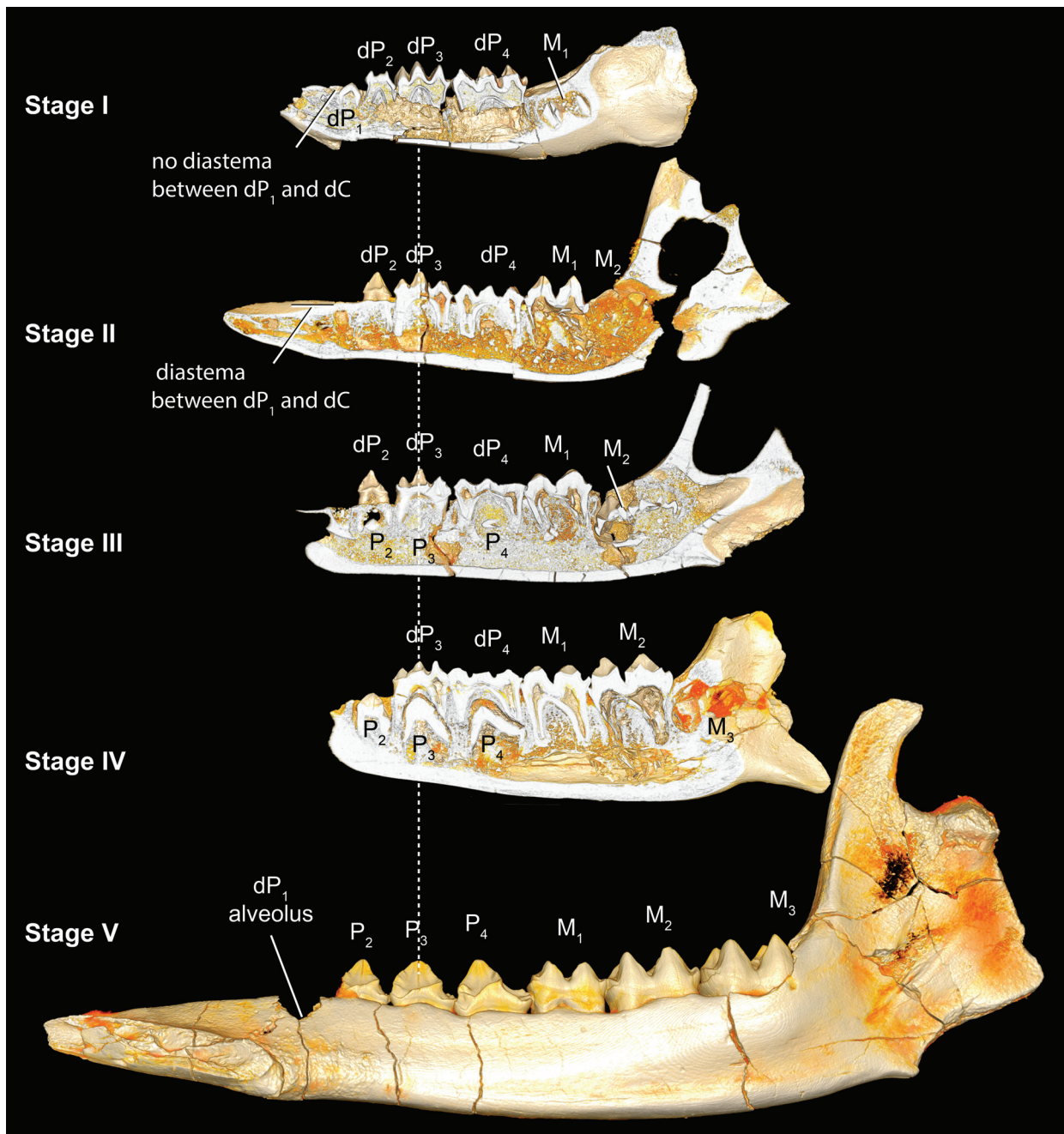


FIGURE 9. Comparison of the different stages (I-V) of the eruption sequence of *Bothriogenys fraasi*.

berg, 1981), members of *Hippopotamus* almost certainly have longer life spans than did members of *Bothriogenys*, and because of this it may benefit members of *Hippopotamus* to have permanent premolars in place to function in conjunction with the molars in a manner different from that of anthracotheres, especially later in their lives. Given the similarity in body size between *Bothriogenys fraasi* and *Sus scrofa*, it is a reasonable assumption that *Bothriogenys* probably reached reproductive age

by the middle of the second year of life and had a life span of about 12 years (Myers et al., 2016), quite different from that seen in *Hippopotamus* (reproductive age at three and half years and life span of ~55 years).

Examining Laws (1968) *Hippopotamus* groups XII through XX, it is clear that premolars, based on increasing wear, begin to participate in food processing by age 22 and become important alternative agents for processing as molars

become heavily worn. Given that anthracotheres did not live as long as hippos, the permanent premolars were probably less important as alternative food processing agents and may have been more important in food acquisition and initial preparation.

Further evidence that *Hippopotamus* and anthracotheres use their permanent premolars differently can be seen in the wear patterns of premolars versus molars in the two groups. In *Hippopotamus* of advanced age (past the age of 35) all cheek teeth show signs of heavy apical wear such that all teeth become flattened and dentine becomes exposed on the surface. In anthracotheres (at least in all documented Fayum forms), similar wear can be found on the molars but the permanent premolars never exhibit apical wear and, in fact, seldom exhibit any wear at all except along crest surfaces. Premolars remain lightly worn, even in individuals of advanced age. This suggests that anthracothere premolars were used for initial acquisition and slicing of vegetation but were not employed for crushing and grinding functions.

In sum, new information presented here about the dental eruption sequence of *Bothriogenys fraasi*, and comparisons among *B. fraasi*, *Sus*, and *Hippopotamus*, shows that, at least anthracotheres and hippos, have very different dental emergence sequences as a consequence of having highly divergent life history patterns. This finding suggests that a useful test of the hypothesis that Hippopotamidae and bothriodontine anthracotheres may be closely related (Orliac et al., 2010; Lihoreau et al., 2015) can be executed when more complete juvenile dentitions of relevant anthracotheres and early hippos are found. A growing body of life history studies indicate that taxa in close phylogenetic proximity can be expected to share features of their dental developmental pattern (Tattersall and Schwartz, 1974; Byrd, 1981; Greenwald, 1988; Schwartz et al., 2005; Asher and Lehmann, 2008; Asher and Olbricht, 2009; Bastl et al., 2011; Cianco et al., 2012; Asher, 2013; Bastl and Nagel, 2014; Veitschegger and Sanchez-Villagra, 2015). Therefore, the lack of a shared pattern between *B. fraasi*, the only bothriodont anthracothere for which this information is currently available, and *Hippopotamus*, suggests additional evidence is required to test hypotheses of relatedness between these two groups.

ACKNOWLEDGEMENTS

We are thankful to V. Yarborough for preparing the fossils described here, C. Riddle for provid-

ing access to the fossil collection at the Division of Fossil Primates, Duke Lemur Center and J. Thostenson and C. Crawford (Duke University) for providing access to micro-CT scanning facilities. This research was funded by U.S. National Science Foundation grants BCS-0416164 to E.R. Seiffert (ERS) and E.L. Simons, BCS-0819186 (ERS) and BCS-1231288 to ERS, J.G. Fleagle, G.F. Gunnell, and D.M. Boyer. Funding was also provided by grants from The Leakey Foundation to E.R.S. This is Duke Lemur Center publication #1327 and NSF BCS 1552848 to D.M. Boyer. This paper is a contribution to project BR/121/A3/PALEURAFRICA of the Belgian Science Policy Office.

REFERENCES

- Andrews, C.W. 1906. A descriptive catalogue of the tertiary vertebrata of the Fayum, Egypt. Based on the collection of the Egyptian government in the Geological Museum, Cairo, and on the collection in the British Museum (Natural History).
- Asher, R. J. 2013. Dental eruption in ruminants and other mammals. *Zitteliana*, 31:18.
- Asher, R.J. and Lehmann, T. 2008. Dental eruption in afrotherian mammals. *BMC Biology*, 6:14.
- Asher, R.J. and Olbricht, G. 2009. Dental ontogeny in *Macroscelides proboscideus* (Afrotheria) and *Erinaceus europaeus* (Lipotyphla). *Journal of Mammalian Evolution*, 16:99-115.
- Bärmann, E.V. and Rössner, G.E. 2011. Dental nomenclature in Ruminantia: Towards a standard terminological framework. *Mammalian Biology, Zeitschrift für Säugetierkunde*, 76:762-768.
- Bastl, K.A. and Nagel, D. 2014. First evidence of the tooth eruption sequence of the upper jaw in *Hyaenodon* (Hyaenodontidae, Mammalia) and new information on the ontogenetic development of its dentition. *Paläontologische Zeitschrift*, 88:481-494.
- Bastl, K.A., Morlo, M., and Nagel, D. 2011. Differences in the tooth eruption sequence in *Hyaenodon* ('Creodonta': Mammalia) and implications for the systematics of the genus. *Journal of Vertebrate Paleontology*, 31:181-192.
- Black, C. C. 1978. Anthracotheriida, p. 423-434. In Maglio V.J. and Cooke H.B.S., (eds.), *Evolution of African Mammals*. Harvard University Press, Cambridge.
- Boisserie, J.R. and Lihoreau, F. 2006. Emergence of Hippopotamidae: new scenarios. *Comptes Rendus Palevol*, 5:749-756.
- Boisserie, J.R., Lihoreau, F., Orliac, M., Fisher, R.E., Weston, E.M., and Ducrocq, S. 2010. Morphology and phylogenetic relationships of the earliest known hippopotamids (Cetartiodactyla, Hippopotamidae, Kenyapotaminae). *Zoological Journal of the Linnean Society*, 158:325-366.

- Byrd, K.E. 1981. Sequences of dental ontogeny and calitrichid taxonomy. *Primates*, 22:103-118.
- Ciancio, M.R., Castro, M.C., Galliari, F.C., Carlini, A.A., and Asher, R.J. 2012. Evolutionary implications of dental eruption in *Dasybus* (Xenarthra). *Journal of Mammalian Evolution*, 19:1-8. doi:10.1007/s10914-011-9177-7.
- Ducrocq, S. 1997. The anthracotheriid genus *Bothriogenys* (Mammalia, Artiodactyla) in Africa and Asia during the paleogene: phylogenetical and paleobiogeographical relationships. *Stuttgarter Beitrage zur Naturkunde, B (Geologie und Palaontologie)*, 250:1-44.
- Eisenberg, J.F. 1981. *The Mammalian Radiations*. University of Chicago Press, Chicago.
- Geisler, J.H. and Uhen, M.D. 2003. Morphological support for a close relationship between hippos and whales. *Journal of Vertebrate Paleontology*, 23:991-996.
- Greenwald, N.S. 1988. Patterns of tooth eruption and replacement in multituberculate mammals. *Journal of Vertebrate Paleontology*, 8:265-277.
- Holroyd, P.A., Simons E.L., Bown, T.M., Polly, P.D., and Kraus M.J. 1996. New records of terrestrial mammals from the upper Eocene Qasr el Sagha Formation, Fayum Depression, Egypt. *Palaeovertebrata*, 23:175-192.
- Holroyd, P.A., Lihoreau P., Gunnell G.F., and Miller E.R. 2010. Anthracotheriidae, p. 843-85. In Werdelin L. and Sanders W.J. (eds.), *Cenozoic Mammals of Africa*, University of California Press, Berkeley.
- Kaplan, J. 1992. The age of the Fayum primates as determined by paleomagnetic reversal stratigraphy. *Journal of Human Evolution*, 22:495-503.
- Laws, R.M. 1968. Dentition and ageing of the hippopotamus. *East African Wildlife Journal*, 6:19-52.
- Lihoreau, F., Boisserie, J.R., Manthi, F.K., and Ducrocq, S. 2015. Hippos stem from the longest sequence of terrestrial cetartiodactyl evolution in Africa. *Nature Communications*, 6:6264. doi:10.1038/ncomms7264.
- Lihoreau, F. and Ducrocq, S. 2007. Family Anthracotheriidae, p. 89-105. In Prothero D.R. and Foss S.E. (eds.), *The Evolution of Artiodactyls*. The Johns Hopkins University Press, Baltimore.
- Luckett, W.P. 1993. An ontogenetic assessment of dental homologies in therian mammals, p. 182-204. In Szalay, F.S., Novacek, M.J., and McKenna, M.C. (eds.), *Mammal Phylogeny*, Volume 1. Springer, Berlin.
- Matschke, G.H. 1967. Aging European wild hogs by dentition. *Journal of Wildlife Management*, 31:109-113.
- Miller, E.R., Gunnell, G.F., Abdel Gawad, M., Hamdan, M., El-Barkooky, A.N., and Clementz, M.T. 2014. Anthracotheres from Wadi Moghra, early Miocene, Egypt. *Journal of Paleontology*, 88:967-981.
- Myers, P., Espinosa, R., Parr, C.S., Jones, T., Hammond, G.S., and Dewey, T.A. 2016. The Animal Diversity Web (online). Accessed at animaldiversity.org.
- O'Leary M.A., Patel B.A., and Coleman M.N. 2012. Endocranial petrosal anatomy of *Bothriogenys* (Mammalia, Artiodactyla, Anthracotheriidae), and petrosal volume and density comparison among aquatic and terrestrial artiodactyls and outgroups. *Journal of Paleontology*, 86:44-50.
- Orliac, M., Boisserie, J.R., Lihoreau, F., and MacLatchy, L. 2010. Early Miocene hippopotamids (Cetartiodactyla) constrain the phylogenetic and spatiotemporal settings of hippopotamid origin. *Proceedings of the National Academy of Sciences, USA*, 107:11871-11876.
- Pickford, M. 1991. Revision of the Neogene Anthracotheriidae of Africa. p. 1491-1525. In Salem M.J. (ed.), *The Geology of Libya*. Elsevier, Amsterdam.
- Pickford, M. 2006. Sexual and individual morphometric variation in *Libycosaurus* (Mammalia, Anthracotheriidae) from the Maghreb and Libya. *Geobios*, 39:267-310.
- Pickford, M. 2007. A new suiform (Artiodactyla, Mammalia) from the Early Miocene of East Africa. *Comptes Rendus Palevol*, 6:221-229.
- Pickford, M. 2008. *Libycosaurus petrocchii* Bonarelli, 1947, and *Libycosaurus anisae*, Black, 1972 (Anthracotheriidae, Mammalia): Nomenclatural and geochronological implications. *Annales de Paléontologie*, 94:39-55.
- Schmidt, M. 1913. Ueber Paarhufer der fluviomarinen Schicht des Fajum, odontographisches und osteologisches Material. *Geologische und Paläontologische Abhandlungen*, 15:153-264.
- Schwartz, G.T., Mahoney, P., Godfrey, L.R., Cuzzo, F.B., Jungers, W.L., and Randria, G.F.N. 2005. Dental development in *Megaladapis edwardsi* (Primates, Lemuriformes): Implications for understanding life history variation in subfossil lemurs. *Journal of Human Evolution*, 49:702-721.
- Seiffert, E.R. 2006. Revised age estimates for the later Paleogene mammal faunas of Egypt and Oman. *Proceedings of the National Academy of Sciences, USA*, 103:5000-5005.
- Seiffert, E.R. 2012. Early primate evolution in Afro-Arabia. *Evolutionary Anthropology*, 21: 239-253.
- Seiffert, E.R., Bown, T.M., Clyde, W.C., and Simons, E.L. 2008. Geology, paleoenvironment, and age of Birket Qarun Locality 2 (BQ-2), Fayum Depression, Egypt. p. 71-86. In Fleagle J.G. and Gilbert C.C. (eds.), *Elwyn L. Simons: A Search for Origins*, Springer, New York.
- Seiffert, E.R., Simons, E.L., Boyer, D.M., Perry, J.M.G., Ryan, T.M., and Sallam, H.M. 2010. A fossil primate of uncertain affinities from the earliest late Eocene of Egypt. *Proceedings of the National Academy of Sciences*, 107:9712-9717
- Sileem, A.H., Sallam, H.M., Hewaidy, A.A., Gunnell, G.F., and Miller, E.R. 2015. Anthracotheres (Mammalia, Artiodactyla) from the upper-most horizon of the Jebel Qatrani Formation, latest early Oligocene, Fayum Depression, Egypt. *Egyptian Journal of Paleontology*, 15:1-11.

- Sileem, A.H., Sallam, H.M., Hewaidy, A.A., Miller, E.R., and Gunnell, G.F. 2016. A new anthracothere (Artiodactyla) from the early Oligocene, Fayum, Egypt, and the mystery of African '*Rhagatherium*' solved. *Journal of Paleontology*, 90.1:170-181.
- Simons, E.L. 2008. Eocene and Oligocene mammals of the Fayum, Egypt. p. 87-105. In Fleagle, J.G. and Gilbert, C.C. (eds.), *Elwyn Simons: A Search for Origins*. Springer, New York.
- Simons, E.L. and Rasmussen, D.T. 1990. Vertebrate paleontology of Fayum: history of research, faunal review and future prospects, p. 627-638. In Said, R. (ed.), *The Geology of Egypt*. A.A. Balkema, Rotterdam.
- Smith, B.H. 2000. 'Schultz's Rule' and the evolution of tooth emergence and replacement patterns in primates and ungulates, p. 212-227. In Teaford, M.F., Smith, M.M., and Ferguson, M.W.J. (eds.), *Development, Function and Evolution of Teeth*. Cambridge University Press, Cambridge.
- Tattersall, I. and Schwartz, J.H. 1974. Craniodental morphology and the systematics of the Malagasy lemurs (Primates, Prosimii). *Anthropological Papers of the American Museum of Natural History*, 52:139-192.
- Uhen, M.D. 2000. Replacement of deciduous first premolars and dental eruption in archaeocete whales. *Journal of Mammalogy*, 81:123-133.
- Veitschegger, K. and Sánchez-Villagra, M.R. 2015. Tooth eruption sequences in cervids and the effect of morphology, life history, and phylogeny. *Journal of Mammalian Evolution*. doi: 10.1007/s10914-015-9315-8.
- Zeigler, A.C. 1971. A theory of the evolution of therian dental formulas and replacement patterns. *Quarterly Review of Biology*, 46:226-249.

SUPPLEMENTAL MATERIAL

Scanning information for *Bothriogenys fraasi* specimens used in this study. Cite DOI and specimen number when utilizing scans from this table. All files are available directly from: www.MorphoSource.org.

Specimen	DOI	File size (MB)	File type
DPC-2705	doi.org/10.17602/M2/M13080	2.30 MB	Digital camera image
	doi.org/10.17602/M2/M16982	410.32 MB	Mesh file
	doi.org/10.17602/M2/M12688	502.22 MB	Zipped tiff stack
DPC-3224	doi.org/10.17602/M2/M13082	2.56 MB	Digital camera image
	doi.org/10.17602/M2/M16983	47.15 MB	Mesh file
	doi.org/10.17602/M2/M12690	77.86 MB	Zipped tiff stack
DPC-3606	doi.org/10.17602/M2/M13075	2.68 MB	Digital camera image
	doi.org/10.17602/M2/M16986	761.77 MB	Mesh file
	doi.org/10.17602/M2/M12653	779.97 MB	Zipped tiff stack
DPC-3947	doi.org/10.17602/M2/M13060	2.71 MB	Digital camera image
	doi.org/10.17602/M2/M17001	153.51 MB	Mesh file
	doi.org/10.17602/M2/M12639	259.23 MB	Zipped tiff stack
DPC-4894	doi.org/10.17602/M2/M13063	2.68 MB	Digital camera image
	doi.org/10.17602/M2/M17002	256.65 MB	Mesh file
	doi.org/10.17602/M2/M12644	206.21 MB	Zipped tiff stack
DPC-5167	doi.org/10.17602/M2/M13066	2.64 MB	Digital camera image
	doi.org/10.17602/M2/M17003	163.21 MB	Mesh file
	doi.org/10.17602/M2/M12646	275.07 MB	Zipped tiff stack
DPC-6147	doi.org/10.17602/M2/M13070	2.56 MB	Digital camera image
	doi.org/10.17602/M2/M17004	43.24 MB	Mesh file
	doi.org/10.17602/M2/M12649	363.82 MB	Zipped tiff stack
DPC-6207	doi.org/10.17602/M2/M17033	2.74 MB	Digital camera image
	doi.org/10.17602/M2/M17031	2.740 GB	Mesh file
	doi.org/10.17602/M2/M17032	769.88 MB	Zipped tiff stack
DPC-7706	doi.org/10.17602/M2/M17037	2.72 MB	Digital camera image
	doi.org/10.17602/M2/M17035	217.59 MB	Mesh file
	doi.org/10.17602/M2/M17034	513.22 MB	Zipped tiff stack
DPC-7730	doi.org/10.17602/M2/M13078	2.30 MB	Digital camera image
	doi.org/10.17602/M2/M17029	298.16 MB	Mesh file
	doi.org/10.17602/M2/M12655	435.92 MB	Zipped tiff stack
DPC-8638	doi.org/10.17602/M2/M13079	2.75 MB	Digital camera image
	doi.org/10.17602/M2/M17030	270.24 MB	Mesh file
	doi.org/10.17602/M2/M12684	202.75 MB	Zipped tiff stack
DPC-10616	doi.org/10.17602/M2/M13071	2.70 MB	Digital camera image
	doi.org/10.17602/M2/M16969	456.16 MB	Mesh file
	doi.org/10.17602/M2/M12650	614.44 MB	Zipped tiff stack
DPC-10633	doi.org/10.17602/M2/M13076	2.64 MB	Digital camera image
	doi.org/10.17602/M2/M16963	573.96 MB	Mesh file

Specimen	DOI	File size (MB)	File type
	doi.org/10.17602/M2/M12654	732.29 MB	Zipped tiff stack
	doi.org/10.17602/M2/M13084	2.64 MB	Digital camera image
DPC-10677	doi.org/10.17602/M2/M16966	500.91 MB	Mesh file
	doi.org/10.17602/M2/M12698	436.46 MB	Zipped tiff stack
	doi.org/10.17602/M2/M13065	2.65 MB	Digital camera image
DPC-11280	doi.org/10.17602/M2/M16970	215.02 MB	Mesh file
	doi.org/10.17602/M2/M12645	235.51 MB	Zipped tiff stack
	doi.org/10.17602/M2/M13074	2.71 MB	Digital camera image
DPC-11407	doi.org/10.17602/M2/M16971	559.86 MB	Mesh file
	doi.org/10.17602/M2/M12651	782.23 MB	Zipped tiff stack
	doi.org/10.17602/M2/M13068	2.74 MB	Digital camera image
DPC-11412	doi.org/10.17602/M2/M16972	422.1 MB	Mesh file
	doi.org/10.17602/M2/M12648	511.58 MB	Zipped tiff stack
	doi.org/10.17602/M2/M13062	2.61 MB	Digital camera image
DPC-11416	doi.org/10.17602/M2/M16974	225.28 MB	Mesh file
	doi.org/10.17602/M2/M12641	282.98 MB	Zipped tiff stack
	doi.org/10.17602/M2/M13059	2.77 MB	Digital camera image
DPC-13562	doi.org/10.17602/M2/M16975	351.17 MB	Mesh file
	doi.org/10.17602/M2/M12638	443.05 MB	Zipped tiff stack
	doi.org/10.17602/M2/M17042	2.98 MB	Digital camera image
DPC-13570	doi.org/10.17602/M2/M17039	234.05 MB	Mesh file
	doi.org/10.17602/M2/M17038	325.26 MB	Zipped tiff stack
	doi.org/10.17602/M2/M13067	2.63 MB	Digital camera image
DPC-20439	doi.org/10.17602/M2/M16979	492.04 MB	Mesh file
	doi.org/10.17602/M2/M12647	723.26 MB	Zipped tiff stack